Available online at www.sciencedirect.com
SCIENCE DIRECT®
Polymer 44 (2003) 6873–6882
polymer
www.elsevier.com/locate/polymer

Thermal behavior and specific interaction in high glass transition temperature PMMA copolymer

Shiao-Wei Kuo, Hsin-Ching Kao, Feng-Chih Chang*

Institute of Applied Chemistry, National Chiao Tung University, 30050 Hsin-chu, Taiwan, ROC

Received 5 June 2003; received in revised form 28 July 2003; accepted 20 August 2003

Abstract

A series of high glass transition temperature copolymers based on poly(methyl methacrylate) (PMMA) were prepared by free radical copolymerization of methacrylamide and methyl methacrylate monomers in dioxane solvent. The thermal properties and hydrogen-bonding interactions of these poly(methacrylamide-*co*-methyl methacrylate) (PMAAM-*co*-PMMA) copolymers with various compositions were investigated by differential scanning calorimetry (DSC), Fourier transform infrared (FTIR) spectroscopy, and solid-state nuclear magnetic resonance (NMR) spectroscopy. A large positive deviation in the behavior of T_g, based on the Kwei equation from DSC analyses, indicates that strong hydrogen bonding exists between these two monomer segments. The FTIR and solid-state NMR spectroscopic analyses give positive evidence for the hydrogen-bonding interaction between the carbonyl group of PMMA and the amide group of PMAAM (e.g. by displaying significant changes in chemical shifts). Furthermore, the proton spin–lattice relaxation time in the rotating frame ($T_{1\rho}$(H)) has one single value over the entire range of compositions of copolymers, and gives a value shorter than the average predicted. The proton relaxation behavior indicates the rigid nature of the copolymer.

Keywords: Poly(methyl methacrylate); Specific interaction; Copolymer

1. Introduction

The glass-transition temperature (T_g) is an important intrinsic characteristic that influences the material properties of a polymer and its potential applications. Furthermore, polymers with high glass-transition temperatures are attractive for industrial polymer science because of strong economic rewards that may arise from their potential applications. For example, poly(methyl methacrylate) (PMMA) is a transparent polymeric material possessing many desirable properties, such as light weight, high light transmittance, chemical resistance, colorlessness, resistance to weathering corrosion, and good insulating properties [1]. The glass-transition temperature of PMMA, however, is relatively low at about 100 °C, which limits its applications in the optical-electronic industry, for materials such as compact discs (CD), optical glasses, and optical fibers, because it undergoes distortion when used in an inner glazing material [2,3]. In order to raise T_g, the incorporation through copolymerization of rigid or bulky monomer structures within poly(methyl methylacrylate) has been widely reported to overcome the miscibility problem [4,5]. The achieved T_g, however, is usually lower than the Fox rule. Here, we offer a novel approach to raise the value of T_g of PMMA through copolymerization with methacrylamide (MAAM) that relies on the strong hydrogen bonding interactions that exist between these two monomer segments. In this study, we choose the copolymerization of MMA with MAAM, rather than preparing a simple polymer blend of PMMA with PMAAM, for two reasons: (1) a simple miscible polymer blend still has the phase-separation problem at high polymer processing temperatures because of the lower critical solution temperature (LCST), and (2) it has been widely reported that the T_g of the copolymer generally is higher than the corresponding polymer blend because of heterogeneities in the composition of hydrogen-bonded copolymers [6,7]. This result can be explained reasonably by the differences in degrees of rotational freedom caused by intramolecular screening and spacing effects [8]. This phenomenon can also be interpreted in

* Corresponding author. Tel.: +886-35727077; fax: +886-35719507.
E-mail address: changfc@cc.nctu.edu.tw (F.C. Chang).

0032-3861/$ - see front matter © 2003 Published by Elsevier Ltd.
doi:10.1016/j.polymer.2003.08.026

terms of the correlation hole effect described by De Gennes [9].

Poly(methacrylamide) has an amide functional group ($CONH_2$) in the side chain instead of the $COOCH_3$ unit present in PMMA. The NH_2 group can interact with other functional groups, such as ethers and esters, acrylate through hydrogen bonding. Therefore, we expect that hydrogen bonding will exist in PMAAM-*co*-PMMA copolymers between the carbonyl groups of MMA units and the amide groups of MAAM units. The stretching of the carbonyl groups monitored by Fourier transform infrared (FTIR) spectroscopy is an excellent probe to detect molecular interactions between the components of polymers [10–14]. In addition to infrared spectroscopy, solid-state nuclear magnetic resonance (NMR) spectroscopy also provides a powerful tool for monitoring the specific interactions, miscibility, domain size, and molecular mobility resulting from hydrogen bond formation [15–20]. The ^{13}C NMR chemical shifts and line shapes of carbon atom resonances in cross-polarization and magic-angle spinning (CP/MAS) spectra can identify the chemical environments of the carbon atoms in the blend and copolymer since the chemical shift and the line shape are highly sensitive to the local electron density. If a specific interaction affects the local electron density, a change in chemical shift should be observed. Furthermore, the spin–lattice relaxation time in the rotating frame ($T_{1\rho}(H)$) is sensitive to the mobility of local polymer chains and its domain size can also be estimated through the spin-diffusion process.

In this study, we have examined the thermal properties of PMAAM-*co*-PMMA copolymers by differential scanning calorimetry (DSC). The effects of hydrogen bonding, domain size, and molecular motion were analyzed using FTIR and solid-state NMR spectroscopies.

2. Experimental

2.1. Materials

Methyl methacrylate and methacrylamide monomers were purchased from Aldrich and were purified, by distillation under vacuum and nitrogen atmosphere, prior to their polymerization. The radical initiator, azobisisobutyronitrile (AIBN), was recrystallized from ethyl alcohol prior to use. 1,4-Dioxane was distilled under vacuum and then used as the solvent in the solution copolymerization experiments.

2.2. Syntheses of poly(methacrylamide-co-methyl methacrylate) copolymers

Solution copolymerization of methyl methacrylate with methacrylamide was carried out in 1,4-dioxane at 80 °C under a nitrogen atmosphere in a glass reaction flask equipped with a condenser. AIBN (1 wt% with respect to monomers) was employed as an initiator. The mixture was stirred for about 24 h, and then poured into excess isopropyl alcohol with vigorous agitation to precipitate the product. The crude copolymer product was purified by redissolving it in 1,4-dioxane and then adding the solution dropwise into a large excess of isopropyl alcohol. This procedure was repeated several times, and then the residual solvent of the final product was removed under vacuum at 70 °C for 1 day to yield the pure white poly(methacrylamide-*co*-methyl methacrylate). The chemical composition of the copolymer was determined by elemental analysis (EA). The chemical structure is shown in Scheme 1.

2.3. Characterization

Molecular weights and molecular weight distributions were determined by gel permeation chromatography (GPC) using a Waters 510 HPLC—equipped with a 410 Differential Refractometer, a UV detector, and three Ultrastyragel columns (100, 500, and 10^3 Å) connected in series in order of increasing pore size—using THF as an eluent at a flow rate of 0.4 ml/min. The molecular weight calibration curve was obtained using polystyrene standards. EA of N, C, and H in the polymers was determined using an auto-elemental analyzer with helium gas as the carrier. The glass-transition temperature of the copolymer was measured using a DSC from DuPont (DSC-9000). The samples were kept at 280 °C for 3 min and then were cooled quickly to 30 °C from the melt of the first scan. The T_g was obtained at the inflection point of the jump heat capacity using a scan rate of 20 °C/min within the temperature range 30–280 °C. All measurements were conducted under a nitrogen atmosphere. Infrared spectra of copolymer films were determined by the conventional KBr disk method. A 1,4-dioxane solution containing the blend was cast onto a KBr disk. The film used in this study was thin enough to obey the Beer–Lambert law. FTIR spectra were recorded on a Nicolet Avatar 320 FT-IR spectrophotometer after 32 scans were collected with a spectral resolution of 1 cm^{-1}. High-resolution solid-state ^{13}C NMR spectroscopic experiments were carried out at room temperature using a Bruker DSX-400 spectrometer operating at resonance frequencies of 399.53 and 100.47 MHz for ^1H and ^{13}C spectra, respectively. The ^{13}C CP/MAS spectra were measured with a 90°

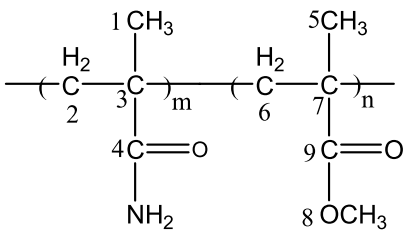

Scheme 1. Chemical structures of PMAAM-*co*-PMMA copolymer and their atom numbering schemes.

pulse of 3.9 μs, a pulse delay time of 3 s, an acquisition time of 30 ms, and a total of 2048 scans. All NMR spectra were taken at 300 K using broad-band proton decoupling and a normal cross-polarization pulse sequence. A magic-angle spinning (MAS) rate of 5.4 kHz was used for the sample to avoid overlapping of absorptions. The proton spin–lattice relaxation time in the rotating frame ($T_{1\rho}$(H)) was determined indirectly by carbon atom observation using a 90°–τ–spin-lock pulse sequence prior to cross-polarization. The data acquisition was performed by ^{1}H decoupling with delay times (τ) ranging from 0.1 to 10 ms and a contact time of 1.0 ms.

3. Results and discussion

3.1. Copolymer analyses

The chemical composition of the copolymer was measured by EA. Good correlations were found between experimental and theoretical predictions of pure PMAAM and pure PMMA. Table 1 lists the MAAM monomer feed ratio, MAAM copolymer composition, and molecular weights. In addition, the reactivity ratios in this study were determined by low conversion (< 10%) of copolymerization PMAAM and PMMA by Eq. (1) using the methodology of Kelen and Tudos [21,22], which we have described previously [23]. The results of this analysis of the PMAAM-*co*-PMMA copolymers are shown graphically in Fig. 1, from which values of $r_{PMAAM} = 0.24$ and $r_{PMMA} = 1.38$ have been calculated. In general, the microstructure of a copolymer can be defined by the distribution of sequence lengths, which can be predicted from the reactivity ratios by the application of statistical relations [24]. For a copolymerization system presenting a predominantly random distribution of monomer units in the copolymer chains, then

$$P_{12} = 1 - P_{11} = \frac{1}{1 + r_1 X} \quad (1)$$

$$P_{21} = 1 - P_{22} = \frac{1}{1 + r_2/X} \quad (2)$$

where P_{ij} is the conditional probability of the addition of monomer j to a growing chain terminated with an active i radical, and $X = [M_1]/[M_2]$ is the composition of the monomer feed.[25] Here, M_1 is the MAAM monomer and M_2 is the MMA monomer, and the calculated values of P_{12} and P_{21}, based on Eqs. (1) and (2), are listed in Table 1. For example, the microstructure of MAAM in the PMAAM39.1 copolymer has a 78% composition of isolated MAAM units, 17.2% of diads, 3.7% of triads, and 0.8% of tetrads ($0.8\% = P_{11}^3 \times P_{12} \times 100\%$ and so on) [26], indicating that the MAAM monomer usually ends up in an isolated single MAAM sequence (M_1) in the PMAAM-*co*-PMMA copolymer. Taking into account the microstructures of these copolymer systems, we know that the intermolecular hydrogen bonding between the carbonyl group of PMMA and the amide group of PMAAM (P_{12}) has a larger probability of occurring than the self-association through hydrogen bonding of pure PMAAM (P_{11}).

3.2. Thermal analysis

Fig. 2 shows the DSC thermograms of pure PMMA, pure PMAAM, and several PMAAM-*co*-PMMA copolymers. The pure PMMA and PMAAM show single glass-transition temperatures at about 100 and 251 °C, respectively. The difference between the chemical structures of PMAAM and PMMA is that the methoxyl groups of PMMA are replaced by amino groups in PMAAM, and this change results in the significant increase in glass-transition temperature because of the formation of strong hydrogen bonds in PMAAM. Single glass-transition temperatures were observed also with the PMAAM-*co*-PMMA copolymers (Table 1), which indicate that these copolymers are homogeneous in the range 10–30 nm [27].

The dependence of the glass-transition temperature on the composition of a polymer blend, and of *block*, *graft*, and

Table 1
Information on poly(methacrylamide-*co*-methyl methacrylate) in this study

Polymer	MAAM (mol%)		P_{12}	P_{21}	M_w	T_g (°C)
	Monomer feed	Polymer composition				
PMMA	0	0	0	0	57,000	100
PMAAM3.7	5.8	3.7	0.99	0.04	53,000	123
PMAAM8.4	11.6	8.4	0.97	0.09	54,000	126
PMAAM13.2	17.2	13.2	0.95	0.13	38,300	144
PMAAM15.0	22.7	15.1	0.93	0.18	23,900	149
PMAAM32.3	44.0	32.3	0.84	0.36	26,400	203
PMAAM39.1	54.0	39.1	0.78	0.46	25,000	212
PMAAM45.2	63.8	45.2	0.70	0.56	26,000	227
PMAAM56.2	82.5	56.1	0.47	0.77	27,000	244
PMAAM	100	100	0	0	11,000	251

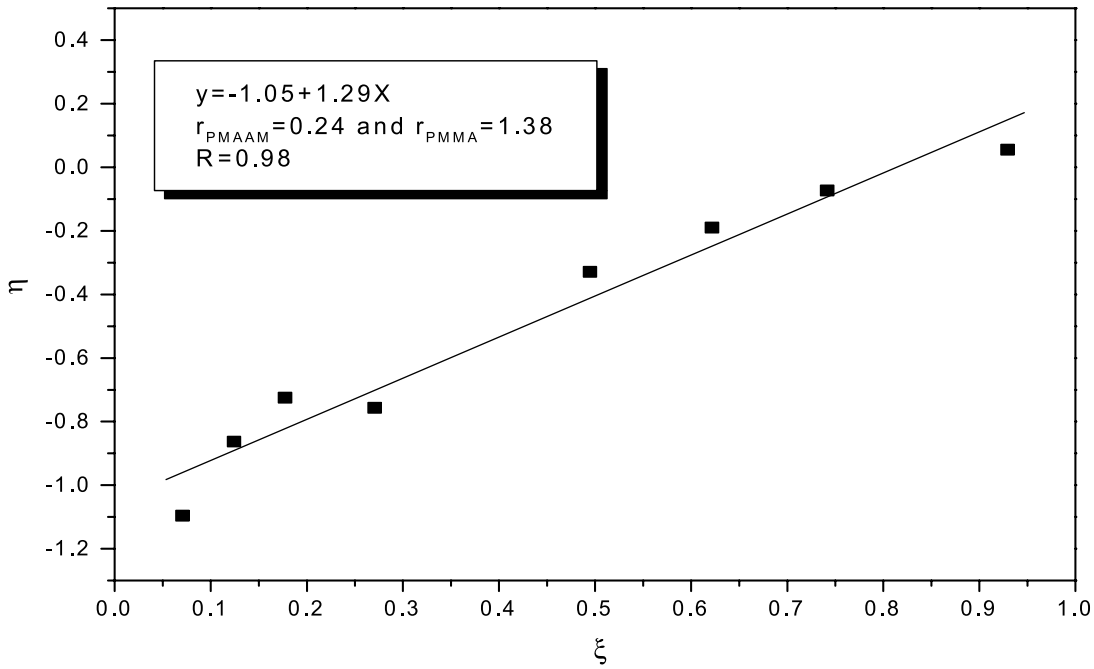

Fig. 1. Kelen–Tudos plot for PMAAM-*co*-PMMA copolymers.

statistical copolymers, has been studied for many systems using the free-volume theory suggested by the Fox rule [28]. There are four possible sequences of diad units in a copolymer formed from monomers M_1 and M_2, namely 11, 22, 12 and 21. Johnston has proposed expanding Fox's suggested treatment of the free-volume theory by assigning individual values of T_g to 11, 22, and 12/21 diads. Johnston derived the equation [29]:

$$\frac{1}{T_g} - \frac{W_1 P_{11}}{T_{g11}} - \frac{W_2 P_{22}}{T_{g22}} = \frac{1}{T_{g12}}(W_1 P_{11} + W_2 P_{22}) \qquad (3)$$

where T_g is the copolymer glass-transition temperature from experimental data, W_1 and W_2, the weight fractions of monomer units M_1 and M_2, T_{g11} and T_{g22}, the glass-

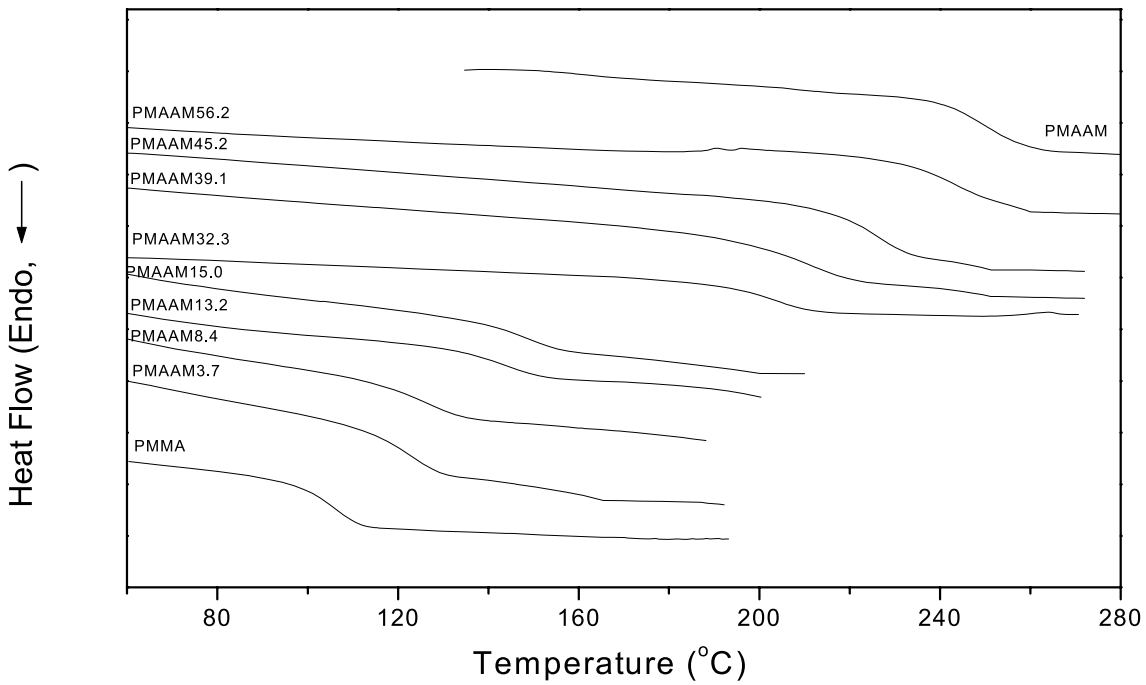

Fig. 2. The DSC scans of PMAAM-*co*-PMMA copolymers.

transition temperatures of both pure homopolymers, and T_{g12} is the glass-transition temperature of the alternating copolymer. Fig. 3 shows that the obtained data can fit the linear relationship of Johnston's treatment (Eq. (3)) of the Fox equation well. From the slopes of the straight lines, we obtain the values of the glass transition temperature of the alternating copolymer (T_{g12}) is 248 °C, which is significantly higher than the pure PMMA. In addition, over the years, many equations have been proposed to extend the Fox equation for the composition dependence of T_g in miscible polymer blends or copolymers, such as those suggested by Gordon–Taylor [30], Couchman [31], and Karasz [32]. Couchman's and Karasz's equations [33], which are based on thermodynamic arguments, have the advantage of being formulated in terms of pure components. Although these equations have been applied successfully to some blends and copolymers, there are still systems where the deviations are significant—particularly those blend systems containing specific interactions [34–37]. The most popular and adequate equation for hydrogen-bonded polymer blends or copolymers is the Kwei equation [38]:

$$T_g = \frac{W_1 T_{g1} + kW_2 T_{g2}}{W_1 + kW_2} + qW_1 W_2 \quad (4)$$

where W_1 and W_2 are weight fractions of the compositions, T_{g1} and T_{g2} represent the corresponding glass-transition temperatures, and k and q are fitting constants. Where q is a parameter corresponding to the strength of hydrogen bonding in the blend, reflecting a balance between the breaking of the self-association and the forming of the interassociation hydrogen bonding that have been demonstrated by Painter et al. [39]. In addition, the values $k = 1$ and $q = 270$ were obtained from the non-linear least-squares best fit of Eq. (4) (Fig. 4(A)). The positive value of q

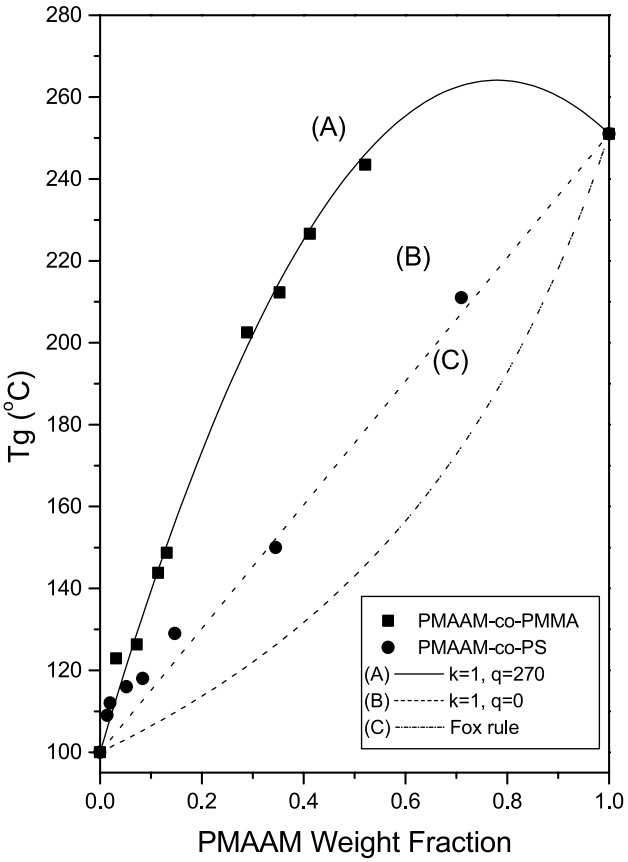

Fig. 4. T_g versus composition curves of PMAAM-*co*-PMMA and PS-*co*-PMAAM copolymers based on experimental data, Fox equation and Kwei equation.

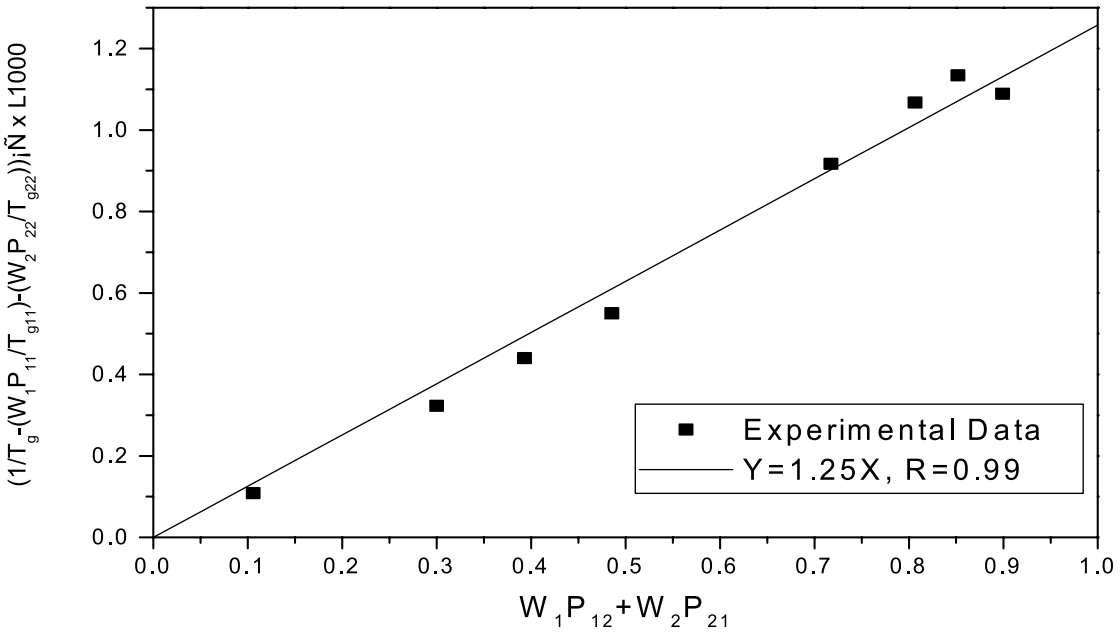

Fig. 3. Application of the linearized expression of Johnston's treatment of the PMAAM-*co*-PMMA copolymers.

indicates a strong intermolecular interaction between MAAM and MMA units. We observe that the Fox rule does not hold well in this PMAAM-*co*-PMMA copolymer because of the strong hydrogen bonding in the copolymer chains (Fig. 4(C)). We note that in a previous study of ours [40], the T_g of PS-*co*-PMAAM copolymer obeys a simple additive rule ($k = 1$, $q = 0$ in Fig. 4(B)), indicating that the PS and PMAAM polymer units in this copolymer system do not exhibit any specific interactions such as hydrogen bonding. Although the pure PS and PMMA homopolymers have the same T_g, significant differences in T_g have been observed when copolymerizing the styrene and MAAM monomers. It is worth noting that incorporating only 32.3 mol% of MAAM into the PMAAM-*co*-PMMA copolymer chain increases the T_g by 100 °C relative to pure PMMA.

3.3. FTIR analyses

In view of the chemical structures and the observed results of the thermal analysis, we believe that specific interactions must exist in this copolymer system. FTIR spectroscopy is one of the most powerful tools for identifying and investigating hydrogen bonding in polymers. Fig. 5 shows scale-expanded infrared spectra of pure PMMA, pure PMAAM, and several PMAAM-*co*-PMMA copolymers in the range 1550–1800 cm^{-1} at room temperature. For convenience, the second-derivative spectrum was used to identify the absorption peaks of PMAAM-*co*-PMMA copolymers. Pure PMAAM shows two bands at 1650 and 1600 cm^{-1}, corresponding to the amide I band (C=O stretching) and the amide Π band (N–H bending), respectively. In generally, the amide Π band has an intensity of one-half to one-third of that of the carbonyl absorption band. The carbonyl stretching for the pure PMMA observed at 1730 cm^{-1} corresponds to the free carbonyl groups. In the PMAAM-*co*-PMMA copolymer, the absorption of the amide I group clearly shifts to higher wavenumber with increasing MMA content, together with a decrease in its intensity. Furthermore, the carbonyl stretching vibration of MMA units in PMAAM-*co*-PMMA copolymers with high MAAM content is split into two bands at 1730 and 1718 cm^{-1}, which correspond to absorption by free and hydrogen-bonded carbonyl groups, respectively. Fig. 6 shows scale-expanded (second-derivative) infrared spectra of the PMAAM45.2 copolymer in the range 1550–1750 cm^{-1}. Clearly, the five main minima under zero-point line (dash line) in the second-derivative spectra shown in Fig. 6(A) are observed for (1) the free carbonyl groups of MMA units at 1732 cm^{-1}, (2) the carbonyl groups at 1718 cm^{-1} of MMA units hydrogen-bonded to amide groups, (3) the free amide I groups of MAAM units at 1684 cm^{-1}, (4) the self-associated, hydrogen-bonding amide I groups of MAAM units at 1654 cm^{-1}, and (5) the amide Π band at 1600 cm^{-1}, which can be fitted well to the Gaussian function. Good correlations exist between the experimental spectra and theoretical fitting of the results (Fig. 6(B)). We emphasize that the small valley in the minimum at 1671 cm^{-1} in Fig. 6(A) corresponds to the amide I groups of PMAAM hydrogen bonding intermolecularly to the carbonyl groups of PMMA. For convenience, we combined the signals of both the self and interassociated hydrogen-bonded amide groups of MAAM units for the analysis of the hydrogen-bonded amide groups. Table 2 summarizes the results of the curve fitting of these spectra, and indicates that the fractions of hydrogen-bonded carbonyl groups in PMMA increases with the increase of MAAM content in the copolymer. Table 2 also shows that the absorption of the hydrogen-bonded amide I groups shifts to higher wavenumber with the increase in the MMA content, which implies that some of the self-associated hydrogen-bonded amide groups become interassociated through hydrogen bonding to carbonyl groups of MMA units.

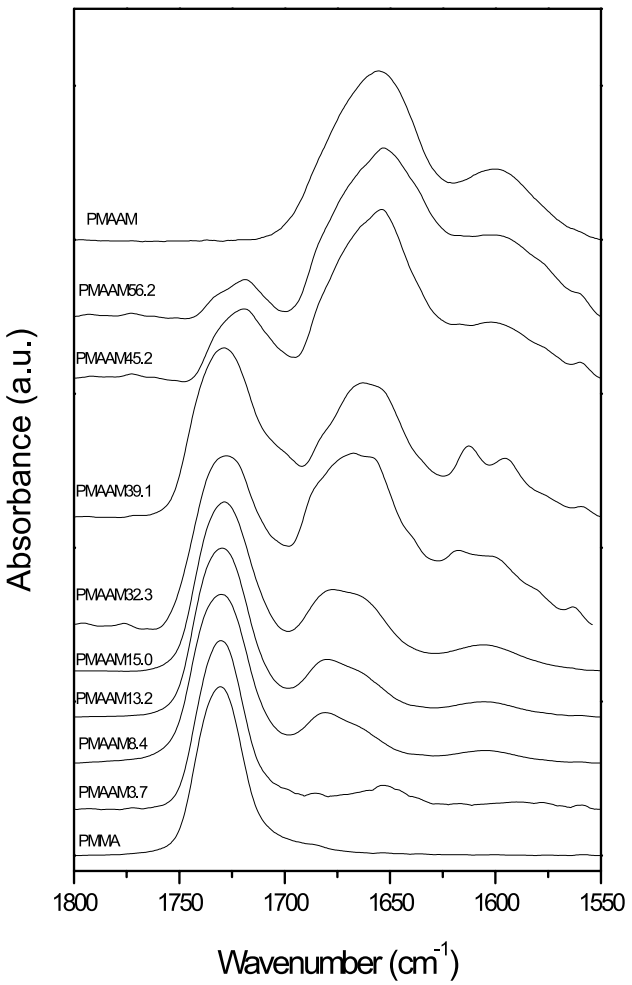

Fig. 5. The IR spectra at 1550–1800 cm^{-1} of pure PMMA, pure PMAAM and PMAAM-*co*-PMMA copolymers with different PMAAM contents at room temperature.

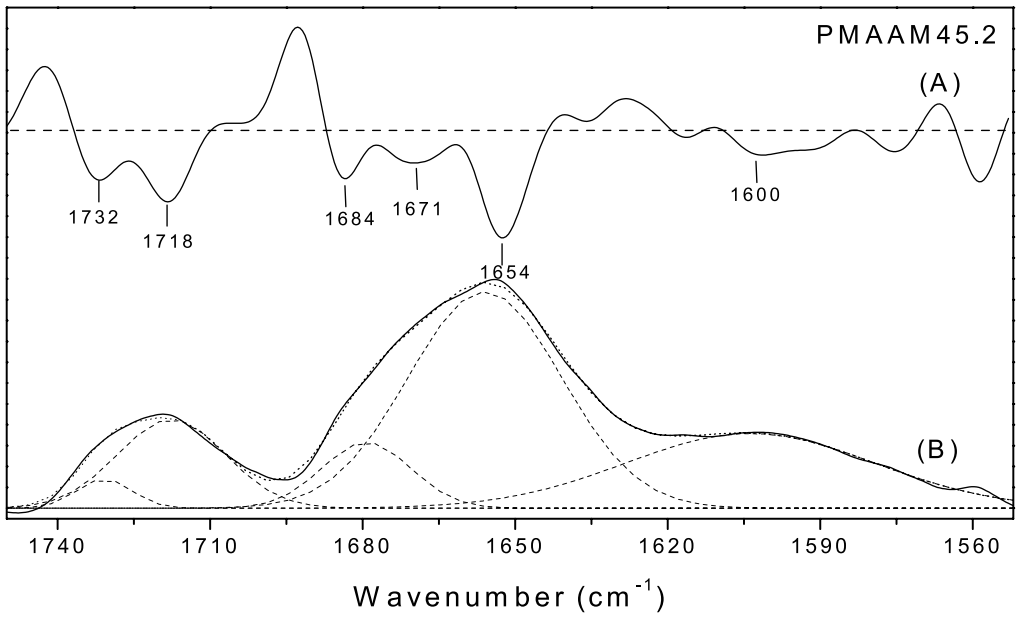

Fig. 6. The IR spectrum at 1550–1800 cm^{-1} and its second derivative spectrum of PMAAM45.2.

3.4. Solid-state NMR analyses

Solid-state NMR spectroscopy provides further insight into the specific interactions, domain sizes, and morphologies of copolymers. The ^{13}C CP/MAS NMR spectra of pure PMAAM and PMMA, and their copolymers, are shown in Fig. 7. The pure PMAAM displays four peaks, and the amide carbon atom is observed at $\delta = 182.5$ ppm. Five peaks are observed for pure PMMA, with the peak at $\delta = 177.9$ ppm coming from the carbonyl carbon atom (C-9). All other peaks designated in Fig. 7 are assigned in Scheme 1. The experimental and simulated data shown in Fig. 7 confirm that the existence of hydrogen-bonding interactions in PMAAM-*co*-PMMA copolymer systems can be determined by solid-state NMR spectroscopy [41]. The simulated spectra of copolymers, shown on the right-hand side, were obtained simply by summing the experimental ^{13}C NMR spectra of pure PMAAM and pure PMMA at the pertinent molar ratio. Clearly, the spectra of the aliphatic region of Fig. 7(B) show a good correlation between the experimental and simulated data. This result implies that there is no specific interaction on the aliphatic region of the copolymer chain. On the contrary, Fig. 7(A) shows that the experimental spectra of PMAAM-*co*-PMMA copolymers differ substantially from the simulated spectra. Complicated experimental spectra were observed, implying that hydrogen bonding exists between the carbonyl groups of PMMA and the amide groups of PMAAM. Fig. 8 shows that the spectrum line widths of most copolymers (carbonyl group + amide group) are larger than those of pure PMAAM, and that the peak of the carbonyl resonance of PMMA (carbonyl group + amide group) shifts significantly downfield with increasing MAAM content in the copolymer, indicating that interactions occur between these two monomer segments. These results are consistent with the FTIR spectroscopic analyses.

Table 2
Curve fitting results of the carbonyl group and amide group in the PMAAM-*co*-PMMA copolymer at room temperature

Polymer	Carbonyl group in PMMA				Amide I group in PMAAM			
	Free C=O		H-bond C=O		Free amide I		H-bond amide I	
	ν (cm^{-1})	A_f (%)	ν (cm^{-1})	A_f (%)	ν (cm^{-1})	A_f (%)	ν (cm^{-1})	A_f (%)
PMMA	1732	100	–	–	–	–	–	–
PMAAM3.7	1735	88	1725	12	ND	ND	ND	ND
PMAAM8.4	1735	75	1725	25	1682	43	1667	57
PMAAM13.2	1734	61	1725	39	1682	34	1667	66
PMAAM15.0	1734	50	1724	50	1682	28	1665	72
PMAAM32.3	1733	40	1721	60	1681	20	1661	80
PMAAM39.1	1733	36	1720	64	1681	17	1658	83
PMAAM45.2	1733	25	1720	75	1681	14	1655	86
PMAAM56.2	1733	22	1719	78	1679	12	1654	88
PMAAM	–	–	–	–	1677	7	1654	93

ND (non-detectable): the signal to noise ratio is too small at lower amide content in PMAAM3.7.

3.5. Analyses of spin–lattice relaxation times in the rotating frame ($T_{1\rho}(H)$)

Previously, ^{13}C spin–lattice relaxation times in the rotating frame ($T_{1\rho}(H)$) have been shown to be sensitive to domain sizes and molecular nobilities in hydrogen bonded polymer blends [42,43]. To the best of our knowledge, no research has been reported to calculate the values of $T_{1\rho}(H)$ in hydrogen-bonded copolymers. In general, the value of

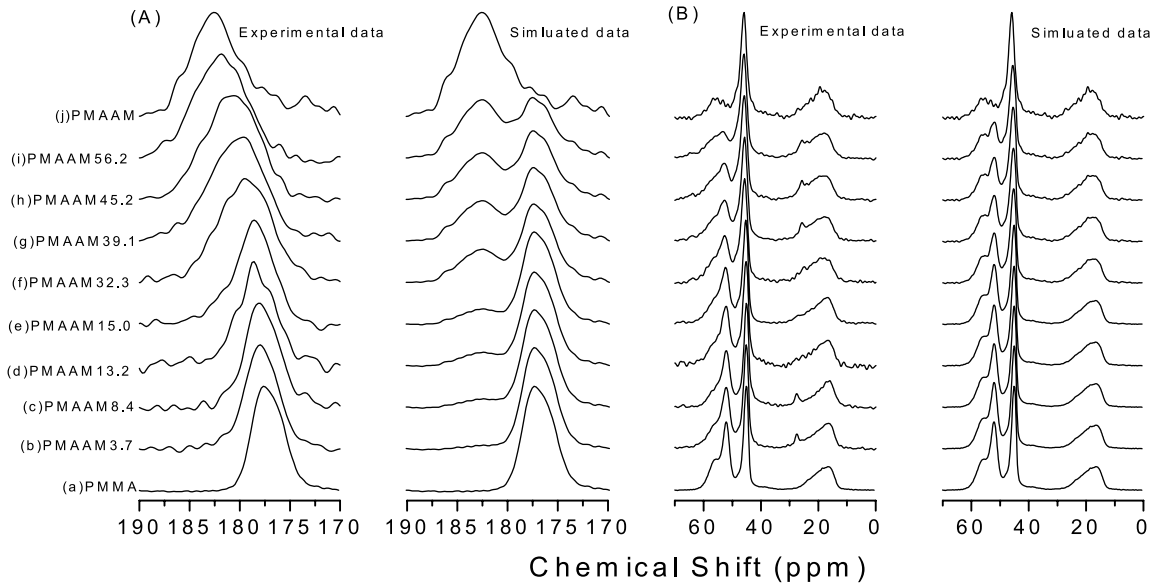

Fig. 7. Experimental and simulated data of ^{13}C CPMAS spectra at room temperature for PMAAM-*co*-PMMA copolymers with different PMAAM contents.

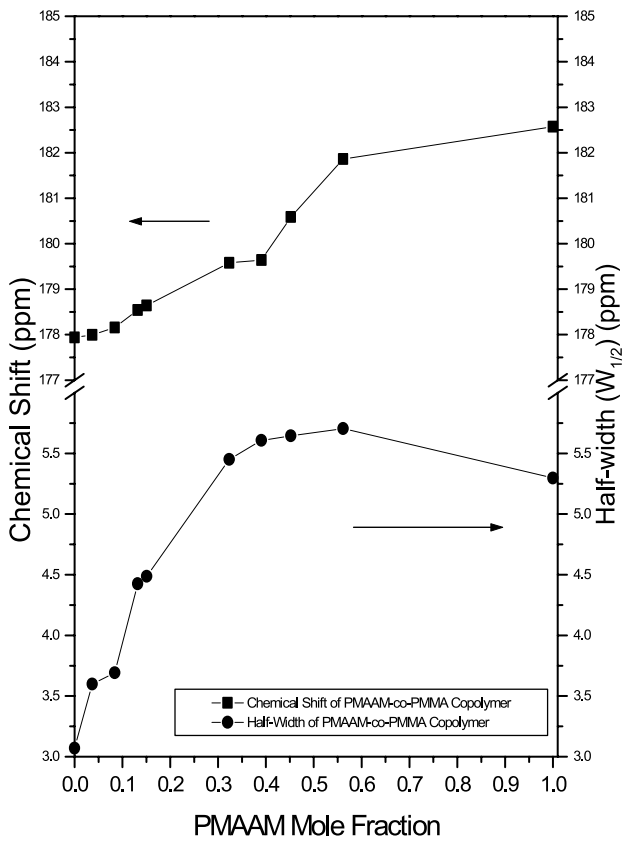

Fig. 8. Chemical shift and half-width of ^{13}C CPMAS spectra at room temperature for PMAAM-*co*-PMMA copolymers with different PMAAM contents.

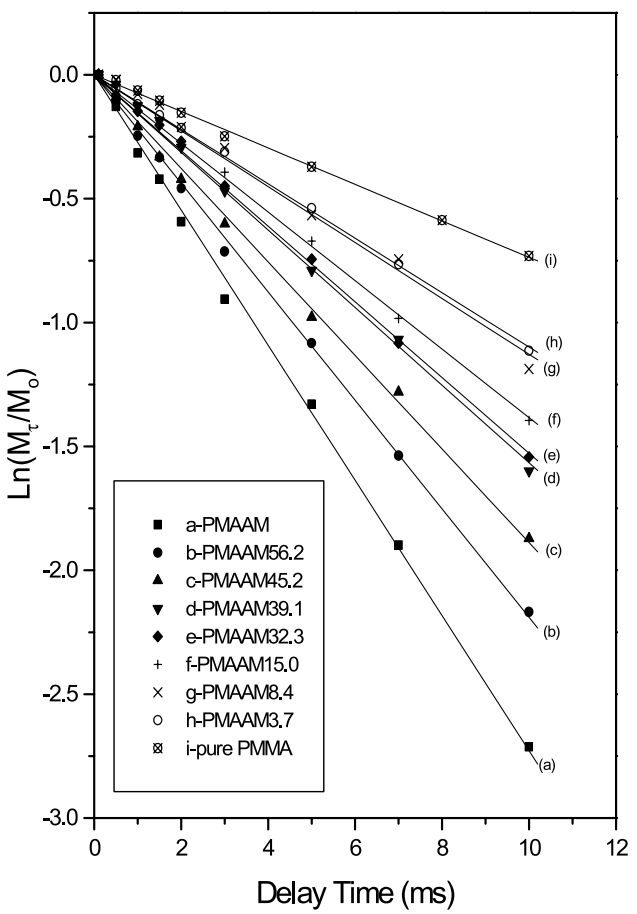

Fig. 9. The semi-logarithmic plots of the magnetization intensities of 45 ppm versus delay time for PMAAM-*co*-PMMA copolymers at contact time of 1 ms.

$T_{1\rho}(H)$ can be calculated from

$$M_\tau = M_0 \exp[-\tau/T_{1\rho}(H)] \quad (5)$$

where τ is the spin-lock time used in the experiment, and M_0 and M_τ are the intensities of peaks at $t = 0$ and τ s, respectively.

Fig. 9 shows the plot of $\ln(M_\tau/M_0)$ versus τ, for the CH_2 carbon atom at $\delta = 45$ ppm for all compositions. The experimental data give a single exponential decay function. The value of $T_{1\rho}(H)$ can be determined from the slope of the plot based on Eq. (5). If a single value of $T_{1\rho}(H)$ is observed in a polymer blend, it means that the dimension of miscibility of the polymer blend is less than 2–3 nm, using the one-dimensional diffusion equation for the average diffusive path length [44]. In this study, this copolymer system is thermodynamically one component and the miscibility of such a system is without any question.

The average proton-relaxation rate of a homogeneous blend or copolymer can be predicted by the model [45,46] of linear additivity of relaxation rates of pure components

$$\frac{1}{T_{1\rho}(H)} = \frac{N_A M_A}{N_T}\left(\frac{1}{T_{1\rho}(H)_A}\right) + \frac{N_B M_B}{N_T}\left(\frac{1}{T_{1\rho}(H)_B}\right) \quad (6)$$

where A and B are components of copolymer segments, M_i, the mole fraction of component i, N_i, the number of protons of component i, $N_T = N_A M_A + N_B M_B$, and $T_{1\rho}(H)_A$ and $T_{1\rho}(H)_B$ denote the relaxation rates of pure components A and B, respectively. Fig. 10 shows the rates of proton relaxation versus the mole fraction of MAAM, both from experimental data and calculated from Eq. (6). For each copolymer composition, the experimental relaxation rate deviates negatively from the calculated value from Eq. (6), suggesting significant excess volume and density changes with various compositions of copolymers [45]. This result reveals that the segmental motion of the copolymer alters significantly and reflects the rigid nature of the copolymer resulting from strong hydrogen bonding.

To confirm the significant excess-volume change in the copolymer chain, we simplify the qualitative analysis of the free-volume change in these copolymer systems by following Kovacs' free-volume theory [47]. According to this theory, the free-volume term can be expressed by

$$f = \Phi_1 f_1 + \Phi_2 f_2 - V_e/V \quad (7)$$

where f is the free volume of the copolymer, f_i and Φ_i, the free volume and the volume fraction of component i, V, the total volume of the blend, V_e, the excess volume, and the term V_e/V is usually related to an interaction term g by means of

$$\frac{V_e}{V} = g\Phi_1\Phi_2 \quad (8)$$

The composition dependence of T_g is given by [48]

$$T_g = \frac{\Phi_2 T_{g2} + K\Phi_1 T_{g1} + (g/\Delta\alpha_2)\Phi_1\Phi_2}{\Phi_2 + K\Phi_1} \quad (9)$$

We can use Eq. (9) to determine the value of g. For convenience, we assume $K = 1$ (i.e. it is equal to the Kwei equation fitting constant ($K = 1$, $q = 270$) and then Eq. (9) becomes the same as the Kwei equation (the volume fraction is used the group contribution method [49] to determine the molar volume). $\Delta\alpha_i$ denotes the difference of the thermal expansion coefficients. Near the T_g, the Simha–Boyer Model [50] can be calculated to obtain the difference in the coefficient of thermal expansion between the glass state and the molten state, as presented in the following

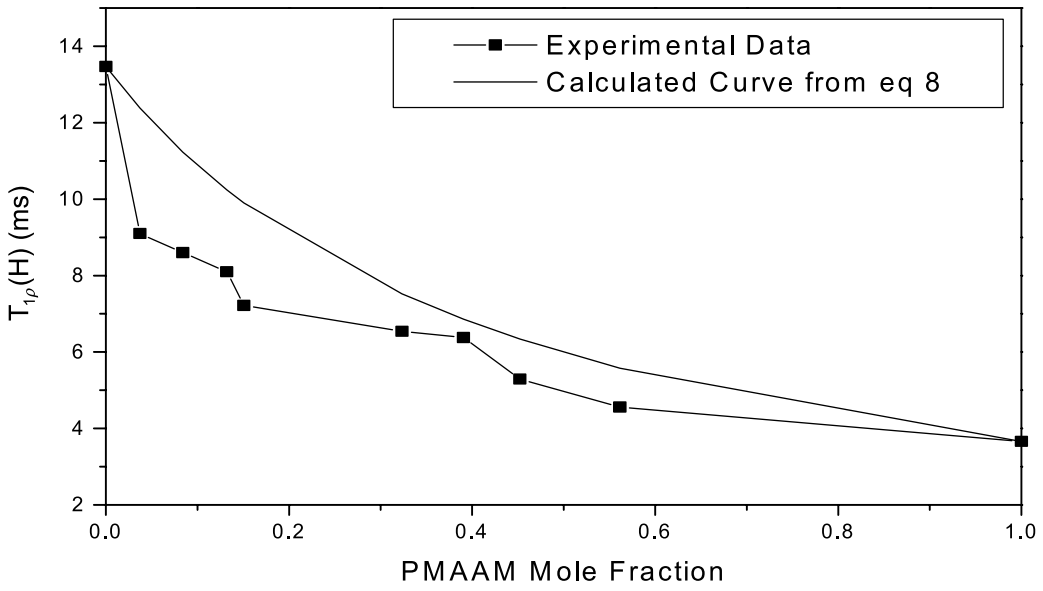

Fig. 10. Plots of $T_{1\rho}(H)$ calculated from Eq. (8) versus different PMAAM contents in PMAAM-*co*-PMMA copolymers.

Eq. (10)

$$\Delta\alpha T_g = 0.115 \quad (10)$$

The value of $\Delta\alpha_2$ could be obtained using the validity of the Simha–Boyer model stating so that $\Delta\alpha_2$ is 3×10^{-4} based on Eq. (10), and the value of g is obtained to be 0.081, implying that a significant excess-volume increase causes a decrease in the free volume in the hydrogen-bonded PMAAM-*co*-PMMA copolymer. Therefore, the dependence of T_g on polymer composition shows a positive deviation predicted by the Kwei equation ($q > 0$).

4. Conclusions

A positive deviation of the dependence of T_g on polymer composition was found based on the Kwei equation owing to strong hydrogen bonding existing in the PMAAM-*co*-PMMA copolymer main chain. Both FTIR and solid-state NMR spectroscopic analyses provide positive evidence for hydrogen bonding interactions in these copolymer systems. From measurements of spin–lattice relaxation times in the rotating frame, a single value was obtained for the copolymer that is lower than that predicted by the linear additivity rule, indicating significant excess-volume changes in copolymer systems. This result is consistent with the Kovacs free-volume theory that significant excess-volume change causes a decrease in the free volume in the hydrogen-bonded PMAAM-*co*-PMMA copolymer. Therefore, a significant increase in T_g of PMMA can be achieved by copolymerization with PMAAM.

Acknowledgements

This research was supported financially by the National Science Council, Taiwan, Republic of China, under Contract No. NSC-91-2216-E-009-018.

References

[1] Yuichi K. J Appl Polym Sci 1997;63:363.
[2] Otsu T, Motsumoto T. Polym Bull 1990;23:43.
[3] Braun D, Czerwinski WK. Makromol Chem 1987;188:2389.
[4] Dong S, Wang Q, Wei Y, Zhang Z. J Appl Polym Sci 1999;72:1335.
[5] Mishra A, Sinha TMJ, Choudhary V. J Appl Polym Sci 1998;68:527.
[6] Coleman MM, Xu Y, Painter PC. Macromolecules 1994;27:127.
[7] Kuo SW, Xu H, Huang CF, Chang FC. J Polym Sci, Polym Phys Ed 2002;40:2313.
[8] Painter PC, Veytsman B, Kumar S, Graf JF, Xu Y, Coleman MM. Macromolecules 1997;30:932.
[9] De Gennes PG. Scaling concept in polymer physics. Ithaca, NY: Cornell University Press; 1979.
[10] Fernandez MJ, Valero M, Martinez DI, Iruin JJ. Polymer 1999;34:28.
[11] Martinez DI, Iruin JJ, Fernandez JMJ. Macromolecules 1995;28:3707.
[12] Cesteros LC, Meaurio E, Katime I. Macromolecules 1993;26:2323.
[13] Prinos A, Dompros A, Panayiotou A. Polymer 1998;39:3011.
[14] Ma CCM, Wu HD, Chu PC, Han TT. Macromolecules 1997;30:5443.
[15] Lau C, Zheng S, Zhong Z, Mi Y. Macromolecules 1998;31:7291.
[16] Hill DJT, Whittaker AK, Wong KW. Macromolecules 1999;32:5285.
[17] Zhang X, Takegoshi K, Hikichi K. Macromolecules 1992;25:2336.
[18] Zhang X, Takegoshi K, Hikichi K. Macromolecules 1991;24:5756.
[19] Jack KS, Whittaker AK. Macromolecules 1997;30:3560.
[20] Qin C, Pires ATN, Belfiore LA. Macromolecules 1991;24:666.
[21] Kennedy JP, Kelen T, Tudos FF. J Polym Sci, Polym Chem Ed 1975; 13:2277.
[22] Kelen T, Tudos FF. Macromol Sci Chem (A) 1975;9:1.
[23] Kuo SW, Chang FC. Polymer 2001;42:9843.
[24] Harwood HJ, Ritchey WMJ. J Polym Sci, Polym Phys Ed 1964;2:601.
[25] San RJ, Madruga EL, del Puerto MA. J Polym Sci, Polym Chem Ed 1983;21:691.
[26] Odian G. Principles of polymerization. New York: Wiley; 1991. p. 470.
[27] Utracki LA. Polymer alloy and blends. Munich, Germany: Hanser Publishers; 1989.
[28] Fox TG. J Appl Bull Am Phys Soc 1956;1:123.
[29] Johnston NW. J Macromol Sci, Macromol Chem 1976;C14:215.
[30] Gordon M, Taylor JS. J Appl Chem 1952;2:493.
[31] Couchman PR. Macromolecules 1991;24:5772.
[32] Couchman PR. Polym Engng Sci 1984;24:135.
[33] Couchman P, Karasz FE. Macromolecules 1978;11:1156.
[34] Kuo SW, Chang FC. Macromolecules 2001;34:5224.
[35] De Meftahi MV, Frechet JMJ. Polymer 1988;29:477.
[36] Yang TP, Pearce EM, Kwei TK. Macromolecules 1989;22:1813.
[37] Wang LF, Pearce EM, Kwei TK. J Polym Sci, Polym Phys Ed 1991; 29:619.
[38] Kwei TK. J Polym Sci, Polym Lett Ed 1984;22:307.
[39] Painter PC, Graf JF, Coleman MM. Macromolecules 1991;24:5630.
[40] Kao HC, Kuo SW, Chang FC. J Polym Res 2003;10:111.
[41] Asano A, Eguchi M, Shimizu M, Kurotsu T. Macromolecules 2002; 35:8819.
[42] Zheng S, Mi Y. Polymer 2003;44:1067.
[43] Hill DJT, Whittaker AK, Wong KW. Macromolecules 1999;32:5285.
[44] Clauss J, Schmidr-Rohr K, Spiess HW. Acta Polym 1993;44:1.
[45] McBriety VJ, Duglass DC, Kwei TK. Macromolecules 1978;11:1265.
[46] Dickson LC, Yang H, Chu CW, Stein RS, Chien JCW. Macromolecules 1987;20:1757.
[47] Kovacs AJ. Adv Polym Sci 1963;3:394.
[48] Braun G, Kovacs AJ. In: Prins JA, editor. Physics of non-crystalline solids. Amsterdam: North Holland; 1965.
[49] Coleman MM, Graf JF, Painter PC. Specific interactions and the miscibility of polymer blends. Lancaster, PA: Technomic Publishing; 1991.
[50] Simha R, Boyer RF. J Chem Phys 1962;37:1003.